

## Sensorless Auto Commissioning of the Position Phase Shift Compensation in Permanent Magnet Machines

المعايرة الآلية للالات الكهربائية الثلاثية التي تحتوي على مغناطيس دائم بدون وجود جهاز لقياس السرعة

Kamel Saleh\*<sup>1</sup> & Mark Sumner<sup>2</sup>

كامل صالح، ومارك سيمنر

<sup>1</sup>Department of Electrical Engineering, Faculty of Engineering & Information Technology, An-Najah National University, Nablus, Palestine. <sup>2</sup>Nottingham University

\*Corresponding Author: kamel.saleh@najah.edu

Received: (28/7/2015), Accepted: (8/5/2016)

### Abstract

An automated self commissioning procedures for sensorless controlled AC drives is described where no prior knowledge of the motor parameters is required. The procedures includes the sensorless automatic calculation of the mechanical parameters of the motor drive passing through the sensorless automatic design of the sensorless speed controller and the mechanical observer and finally the sensorless automatic compensation of the error between the tracked saturation saliency position and the real rotor position in the permanent magnet machines due to the armature reaction based on a new technique depends on injecting a pulse of current in the d\_axis, the change in the current in q\_axis will depend on the error between the saturation saliency position and the real rotor position. This change in I<sub>q</sub> is fed back to an integral controller which will generate an angle to compensate the error in the estimated position. This will increase the torque per volume of the PM machine and protect it from demagnetizing. The paper is introducing experimental results to demonstrate the feasibility of this technique.

**Keywords:** Auto Commissioning, Sensorless, SMPM.

### ملخص

هذه الورقة البحثية تقدم طريقة جديدة والية لعملية المعايرة الذاتية للالات الكهربائية التي يتم التحكم بها بدون استخدام مجسات لقياس سرعة هذه الالات وبدون الحاجة للمعرفة المسبقة عن خصائص هذه الالات الكهربائية تضمن الطريقة المبتكرة حساب المواصف الميكانيكية للالات الكهربائية وتصميم الي للمتحكم الذي يتحكم في سرعة الالة وشدة التيار في الالة عندما تعمل الالة بدون مجس السرعة كما وتقدم هذه الورقة طريقة جديدة والية لتصحيح الخطء في مكان المحرك المستنبت بطريقة غير مباشرة (بدون استخدام مجس السرعة) عند اي لحظة وبين مكان المحرك الحقيقي نتيجة تأثير حمل الالة على مكان الاشباع المغناطيسي للالة بواسطة حقن تيار باتجاه المجال المغناطيسي ومراقبة تأثير هذا التيار على عزم الالة ثم يقوم متحكم خاص بتحويل هذا التأثير ال زاوية تستخدم لمعرفة مكان المحرك الحقيقي و هذا يحسن من كفاءة الالة بشكل ملحوظ ويحمي الالة واخيرا تعرض هذه الورقة لنتائج عملية تم اخذها من مختبرات جامعة نوتنجهام في بريطانيا بعد تطبيق هذه الطريقة على الات كهربائية مختلفة والنتائج تظهر كفاءة هذه الطريقة وملاءمتها للانواع المختلفة من الالات الكهربائية.

**الكلمات المفتاحية:** بدون وجود جهاز لقياس السرعة، المعايرة الالية، لالات الكهربائية الثلاثية التي تحتوي على مغناطيس، بدون وجود جهاز لقياس السرعة.

### Introduction

Sensorless vector control of ac machines drives have been in research for many years. A very promising resulted have been obtained for sensorless speed vector of the ac machines drives both at very low speed and at high speeds as well using both the model based methods and the injection methods (Schauder, 1992. 1054-1061), (Jansen, Lorenz, 1995. 240–247), (Schroedl, 1996. 270-277). Today’s industry has been directed to commercially adapting these sensorless techniques. And so it becomes increasingly important to have techniques for self commissioning of such sensorless AC drives especially that there is some slightly differences between such techniques and those are used in sensed AC drives (Sumner, Asher, 1993). The paper is presenting a technique for self auto commissioning of sensorless drives including sensorless self tuning of the speed controller and the mechanical observer (Lorenz, Van Patten, 1991. 701 – 705). and new technique for self automatic compensation of the error between the saliency tracked position and the real rotor position of the permanent magnetic motors to increase the efficiency of the motor and protect it from demagnetization.

The procedures have been evaluated by testing two different motors called motor B and C with different inertias and different ratings. The saliency that is tracked in both motors is the saturation saliency  $2f_e$  and the rating of motors are:-

**Table (1):** Motors B and C parameters.

| parameter                    | Motor B        | Motor C        |
|------------------------------|----------------|----------------|
| Model                        | 142UMC300CACAA | 115UMC300CACAA |
| Rated torque (Nm)            | 12.2           | 8.1            |
| Stall current (Arms)         | 9.6            | 5.9            |
| Rated power (kW)             | 3.83           | 2.54           |
| R(ph-ph) (Ohms)              | 0.94           | 2.02           |
| L(ph-ph) (mH)                | 8.3            | 11.4           |
| Kt (Nm/Arms)                 | 1.6            | 1.6            |
| Ke (Vrms/krpm)               | 98             | 98             |
| No of Poles                  | 6              | 6              |
| Inertia (Kg m <sup>2</sup> ) | .03            | .09            |

The procedures below are done in sensorless mode through tracking the saturation saliency of permanent magnet motors without the need of encoder at all.

#### Automatic sensorless measure of the moment of inertia

The inertia is calculated by applying a pre known torque to the motor using pulses of  $I_q$  when the motor is under sensorless current control mode and through calculating the estimated speed response of the motor due to this torque, the inertia can be calculated (Sumner, Asher, 1993).

$$Torque = k_t * I_q = J * \frac{d\omega}{dt} \quad (1)$$

Where  $k_t$  is the torque constant,  $I_q$  is the torque current,  $J$  is the moment of inertia and  $\frac{d\omega}{dt}$  is the rate of change of the mechanical speed in rad/s. The responses of two motors due to applying a pre known torques

are shown in Fig.1. The moment of inertia of motor B is approximately  $0.0625 \text{ (kg.m}^2\text{)}$  while it is equal  $0.1128 \text{ (kg.m}^2\text{)}$  for motor C.

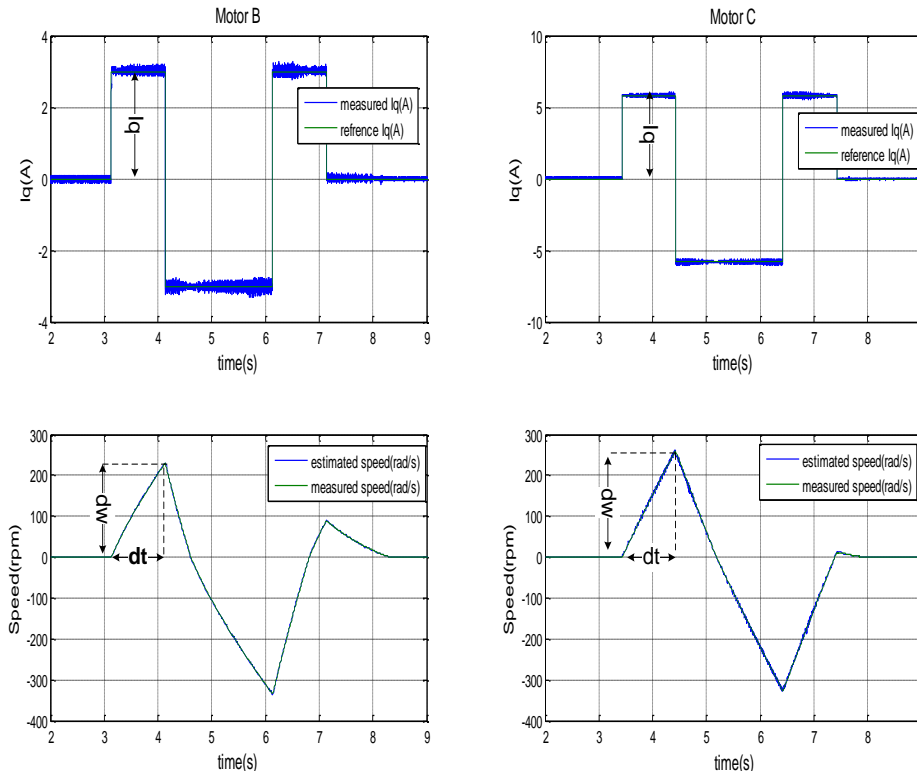


**Figure (1):** Motors response due to applying torque steps.

**Automatic design of the sensorless Speed Controller**

After calculating the moment of inertia for the two motors, these values can be used in designing the sensorless speed controllers. Fig 2 shows both the speed and current loops. From the figure, it can be seen that the value of  $K_p$  of the speed controller determines directly the amplitude of the current ripple (Sumner, Asher, 1993). So a compromising should be done between the bandwidth of the speed controller and the value of  $K_p$ .

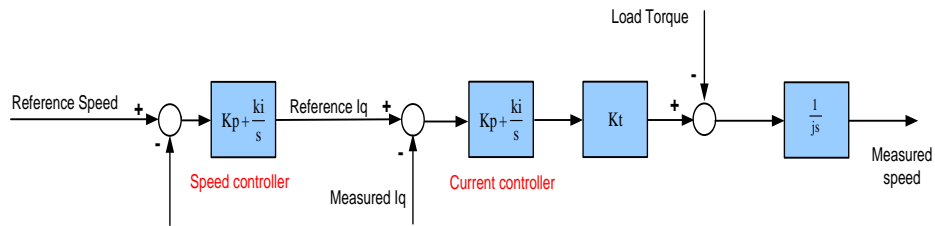


**Figure (2):** Speed and current control loops for vector controlled AC motor.

The closed loop transfer function for the speed loop is :

$$\frac{\text{reference speed}}{\text{measured speed}} = \frac{kt * kp(s + a)}{s^2 + \frac{kt * kp}{J} * s + \frac{kt * kp * a}{J}} \tag{2}$$

Where  $a = \frac{Ki}{Kp}$ . Now suppose that it is desired to have a speed controller with damping factor ( $\zeta$ ) and natural frequency ( $\omega_n$ ), then the denominator of the closed loop should be in the form of  $s^2 + 2 * \zeta * \omega_n s + \omega_n^2$  which means that :-

$$\frac{kt * kp}{J} = 2 * \zeta * \omega_n \tag{3}$$

$$\frac{kt * kp * a}{J} = \omega_n^2 \tag{4}$$

(3) can be rewritten as :-

$$kp = \frac{2 * J * \zeta * \omega_n}{kt} \tag{5}$$

Also (4) can be written as:-

$$a = \frac{\omega_n^2}{J * kp * kt} \tag{6}$$

From (6), the natural frequency ( $\omega_n$ ) can be incremented till the value of  $kp$  equals the value that gives a reasonable performance of the

system. Through experiments, it is found that the value of  $kp$  that give optimal performance is 0.22. Then the value of the natural frequency obtained from (5) is used to calculate  $a$  in (6). This method of automatic design of the sensorless speed controller is illustrated in Fig 22.

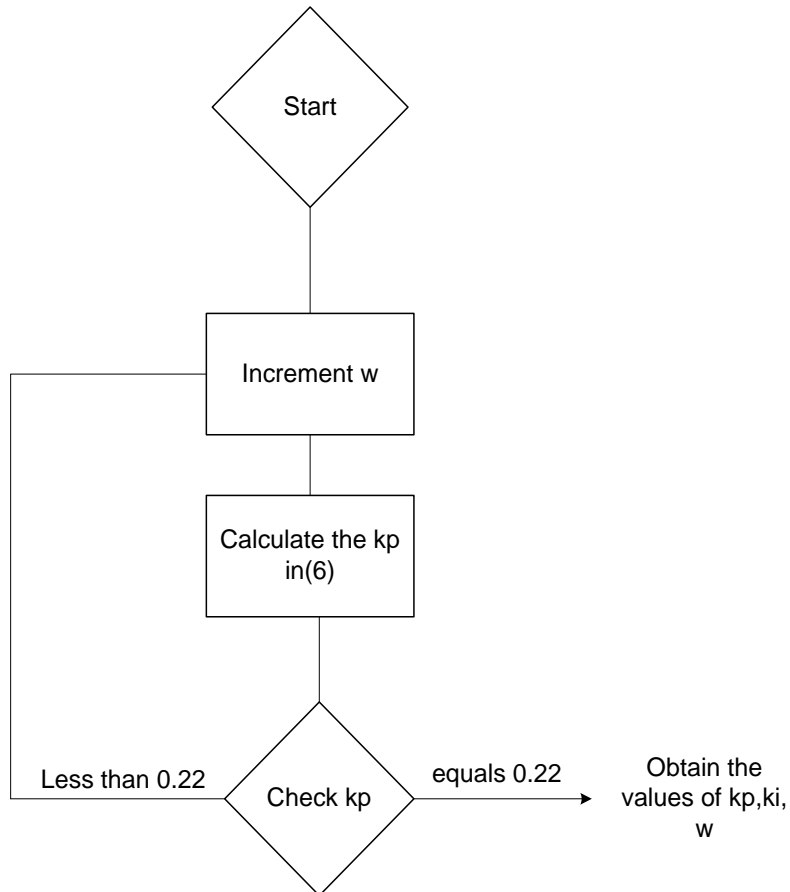


**Figure (3):** Flow chart for automatic design of the speed controller.

Fig 4 shows the root locus and the bode plot of the closed loop speed control for motors B and C obtained using this designing method. More information about the controllers for both motors is given in table 2.

**Table (2):** Speed controller specifications.

|           | Motor B    | Motor C  |
|-----------|------------|----------|
| J         | 0.0625     | 0.1128   |
| $\zeta$   | 0.8        | 0.8      |
| bandwidth | 21.8 rad/s | 12 rad/s |
| Kp        | 0.2187     | 0.219    |
| Ki        | 1.543      | 0.848    |

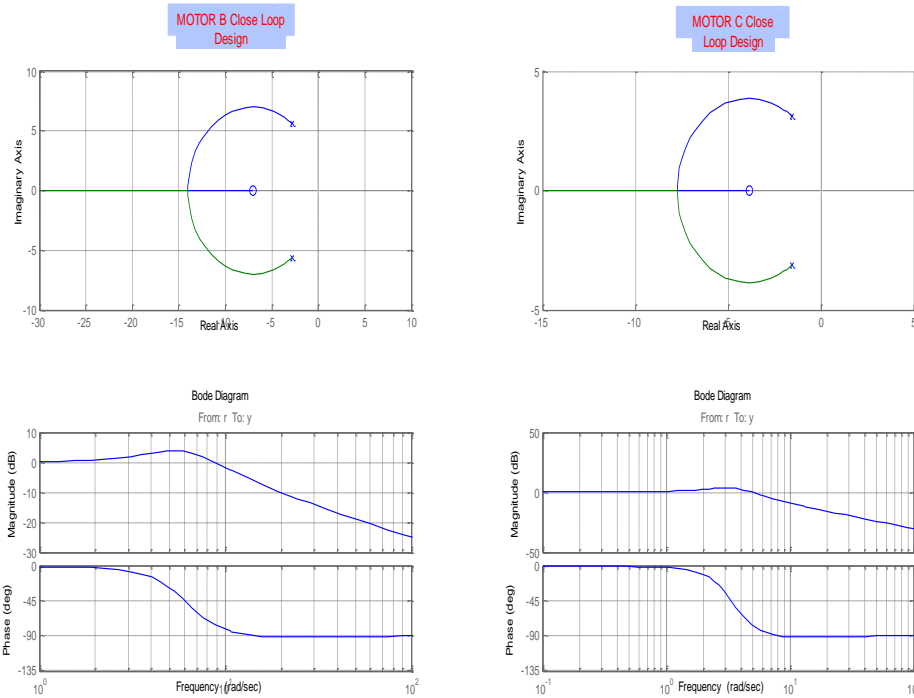


**Figure (4):** root locus and bode plot for the auto designed sensorless speed controllers for motors B and C.

### Automatic Design of the Mechanical Observer

There are two functions for the mechanical observer in the fully sensorless system (Lorenz, Van Patten, 1991. 701 – 705). The first one is to improve the dynamic performance of the estimated speed and position.

And this function requires designing the bandwidth of the controller as much as fast as possible. The other function is to filter out higher frequencies harmonics and noise that may affect the quality of the estimated speed and position at steady state and this requires designing a slower mechanical observer. From the two functions, it is clear that the design of the mechanical observer needs to compromise between the dynamic response of the estimated steady state speed and position qualities.

From experiments, it is found that this compromise can be achieved by designing the bandwidth of the mechanical observer to be 9 times the bandwidth of the speed controller. This will also helps to design the sensorless speed controller and mechanical observer separately as they will not interact with each other.

The closed loop transfer function for the mechanical observer using the PID controller as shown in Fig12 is :-

$$\text{Mechanical Observer CLTF} = \frac{kd * s^2 + kp * s + ki}{J * s^3 + kd * s^2 + kp * s + ki} \quad (7)$$

It is desired to choose values for  $kd$ ,  $kp$  and  $ki$  to make the mechanical observer (7) has the desired bandwidth. To do so, it is more convenient to rewrite the (7) in frequency domain as shown in (13)

$$\text{Mechanical Observer CLTF} = \frac{kd * (j\omega)^2 + kp * (j\omega) + ki}{J * (j\omega)^3 + kd * (j\omega)^2 + kp * (j\omega) + ki} \quad (8)$$

The amplitude of (8) is

$$\frac{\sqrt{(kp * \omega)^2 + (ki - kd * \omega^2)^2}}{\sqrt{(kp * \omega - J * \omega^2)^2 + (ki - kd * \omega^2)^2}} = m \quad (9)$$

For any design of the mechanical observer, if the bandwidth of that design and the controllers parameters are substituted in (9), the amplitude will always equals -6.9 dB. This result is used in this work for automatic design of the mechanical observer. As the value of the bandwidth is already known (9 time the bandwidth of the speed controller), the parameters of the PID controller can be incremented until the amplitude

in (9) equals -6.9 dB. This automatic design of the mechanical observer is illustrated in Fig 5.

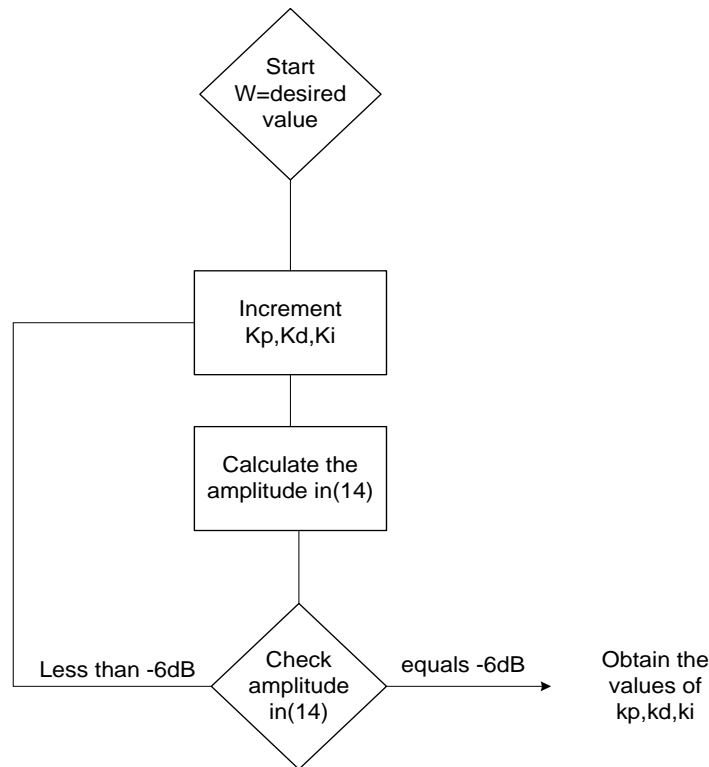


**Figure (5):** Flow chart for automatic design of the mechanical observer.

Fig 6 shows the root locus and the bode plots of the mechanical observer obtained by automatic design of two different imagined motors. From the root locus and the bode plots, it can be seen that the system is stable and also the real bandwidth is almost equals the desired one. The information of the imagined motors is obtained in table 3.

**Table (3):** mechanical observer design specifications.

| Moment of Inertia | Desired Bandwidth (rad/s) | Kd    | Kp    | Ki     |
|-------------------|---------------------------|-------|-------|--------|
| 0.05              | 300                       | 79.45 | 757.5 | 11362  |
| 1.5               | 100                       | 79.45 | 4965  | 744490 |

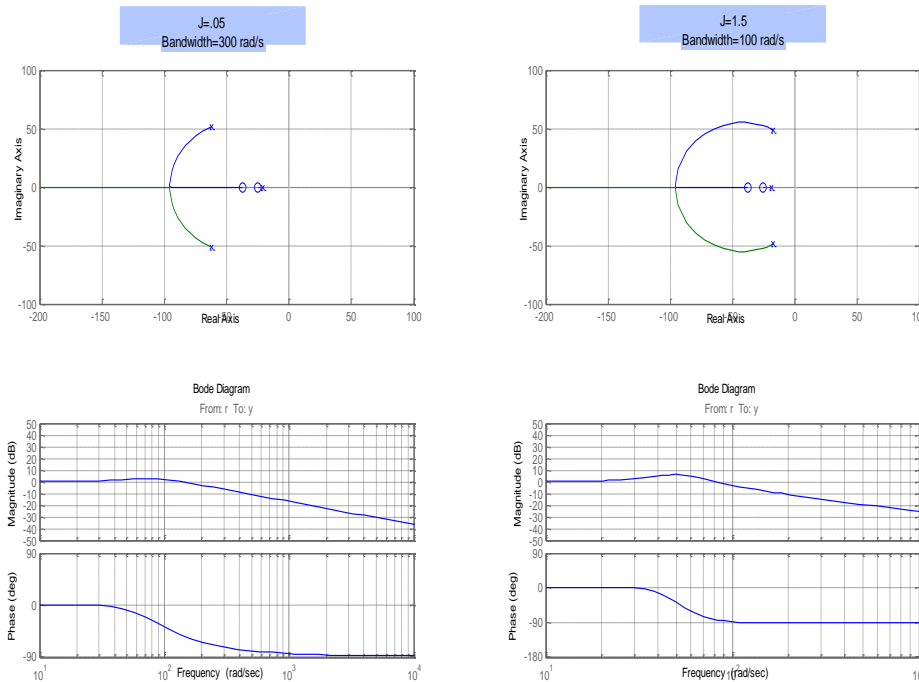


**Figure (6):** root locus and mechanical observer auto designed for different imagined motors.

The evaluation of the automatic calculation of the motor inertia, the automatic design of the speed controller and the automatic design of the mechanical observer are applied on the motors B and C and the results are shown in Fig 7,8. The rms value of the error between the reference speed and the measured speed using the manula design procedure and the automatic design procedures mentioned above gaves almost similar results.

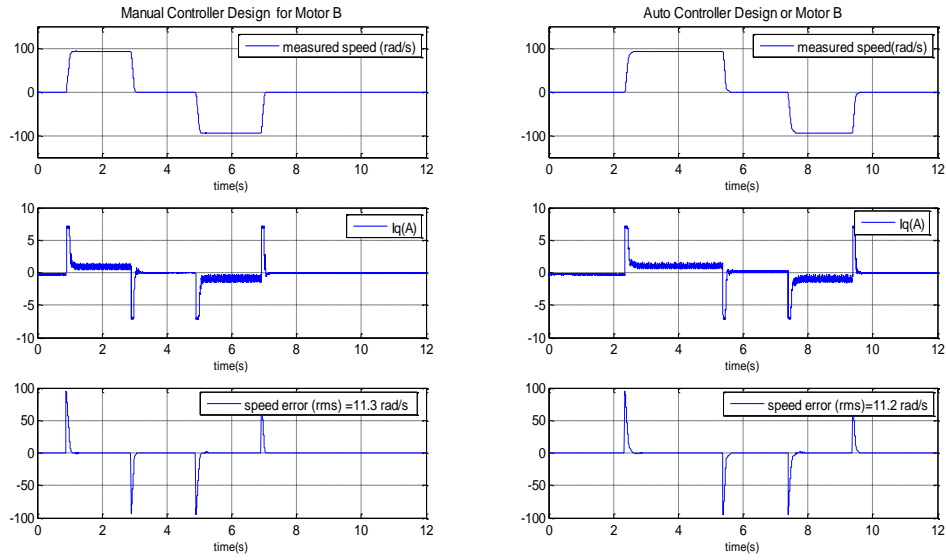


**Figure (7):** Sensorless speed steps at no load for motor B with speed controller and mechanical observer are designed manually and automatically.

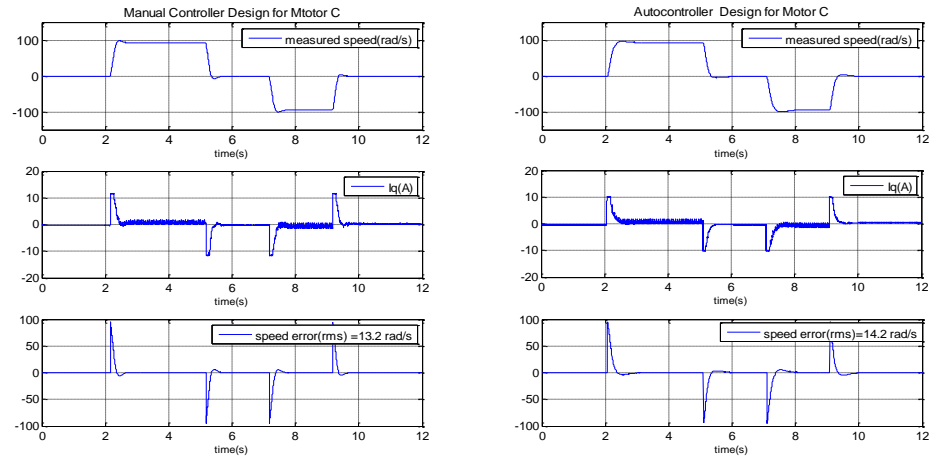


**Figure (8):** Sensorless speed steps at no load for motor C with speed controller and mechanical speed observer are designed manually and automatically.

### Position Error Compensation

The saturation saliency is oriented with the air-gap flux position, instead of the rotor position. The current in the q-axis stator windings creates an additional flux, which deviates the air-gap flux distribution towards the q-axis. The saturation saliency is misaligned from the rotor direction indicated by the d-axis. The spatial shift of the saturation point can be theoretically calculated from:

$$\theta_{shift} = \arctan(L_q I_q / \psi_m) \quad (10)$$

Where  $L_q$  and  $I_q$  are the q-axis inductance and current respectively,  $\psi_m$  is the magnitude of the flux produced by the rotor magnet. (Gao, Asher, Sumner, 2010), (Hua, Asher, Sumner, Gao, 2007. 661-667), (Arias, Sliva, Asher, Clare, Wheeler, 2006). used off line compensation in order to compensate the phase shift error through using lookup tables where the phase shift angle is stored as a function of  $I_q$ . In this method no pre commissioning is needed to compensate the phase shift error as this compensation is done during the normal operation of the PM machine by injecting a pulse of  $I_d$  at rated load and shifting the saliency position till the change in  $I_q$  becomes zero using the similar principals in d-axis injection (Holtz, 2008. 1172–1180), (Ha, Sul, 1997. 426–432), (Corley, Lorenz, 1998. 784–789).

Fig 9 shows experimental results for the error angle between the real rotor position obtained by the encoder and the saliency position as a function of  $I_q$  in a fully sensorless speed control permanent magnet motor in both the motoring and generating modes. The method that is used in this work to track the saliency is the fundamental PWM method and the speed was 100 rpm (5Hz). This phase shift pattern is very weak dependent on the speed. Fig 10. A shows the effect of imposing  $I_d$  pulse at rated load without compensating the phase shift. The change in  $I_q$  due to this injection is clear and the amplitude of this change depends the error between the real rotor position and saliency position.

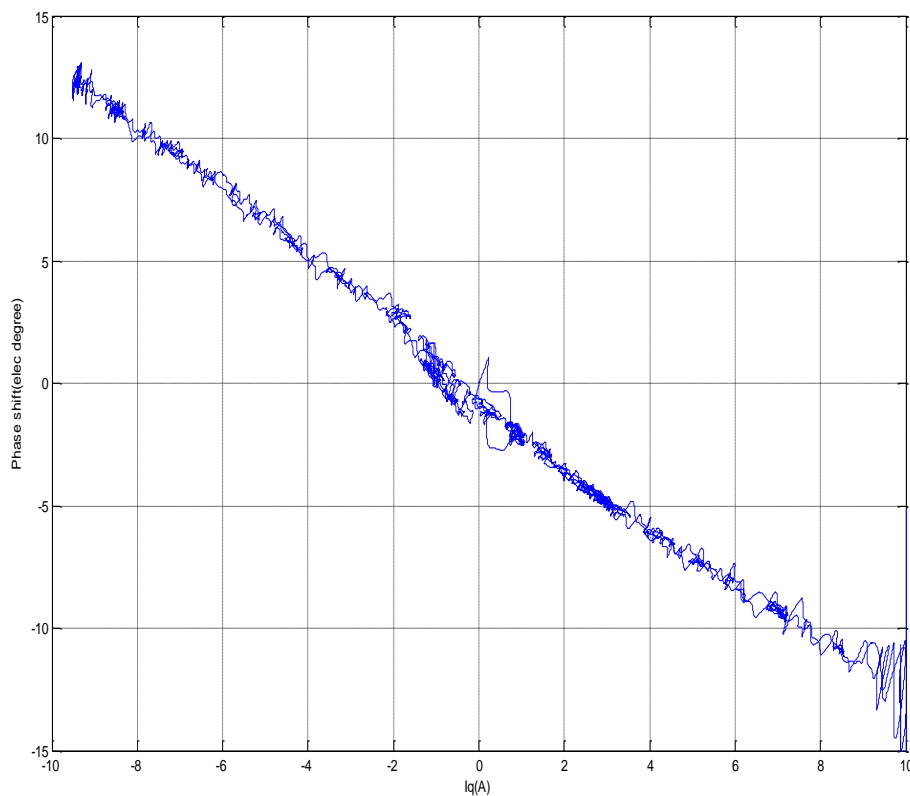


**Figure (9):** shift error between the rotor and saliency position in PM machine.

Fig 10.B illustrates the operation of the new method where  $I_d$  pulse is injected, then the change in  $i_q$  is fed to an integral controller who will generate a compensation angle added to the saliency angle. When the change in  $I_q$  becomes zero this means that the error between the rotor position and saliency position become zero, These value of the compensation angle and the  $I_q$  applied are used to generate a compensation angle at different load conditions according to the following equation:-

$$\theta_{\text{compensated}} = I_q \times \left( \frac{\theta_{\text{compensation}}}{I_q} \right)_{\text{at rated}} \quad (11)$$

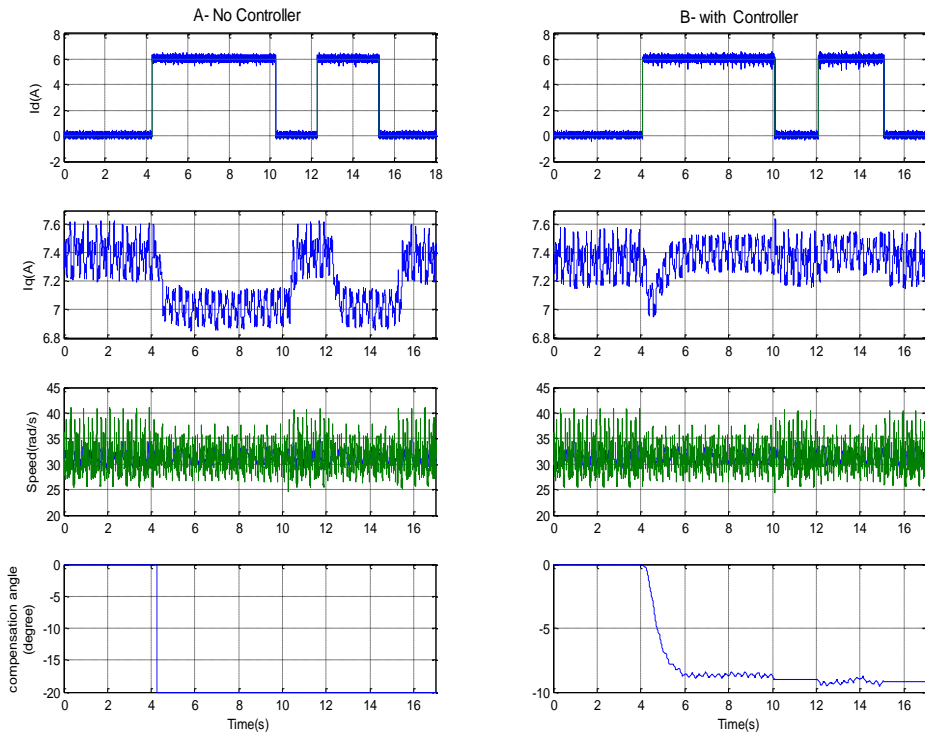


**Figure (10):** Effect of the Injected Id on Iq , A) The phase shift error is not compensated , B) the phase shift error is compensated using integral controller.

Fig 11 shows position error between the tracked saliency and real rotor position at different values of Iq in both motoring and generating modes without compensation this error. Fig 12 shows the same test done but with using (11) to compensate the phase shift. It can be seen clearly that the phase shift has been almost compensated. This is also clear from fig 13 which shows that the error is almost zero rated Iq.

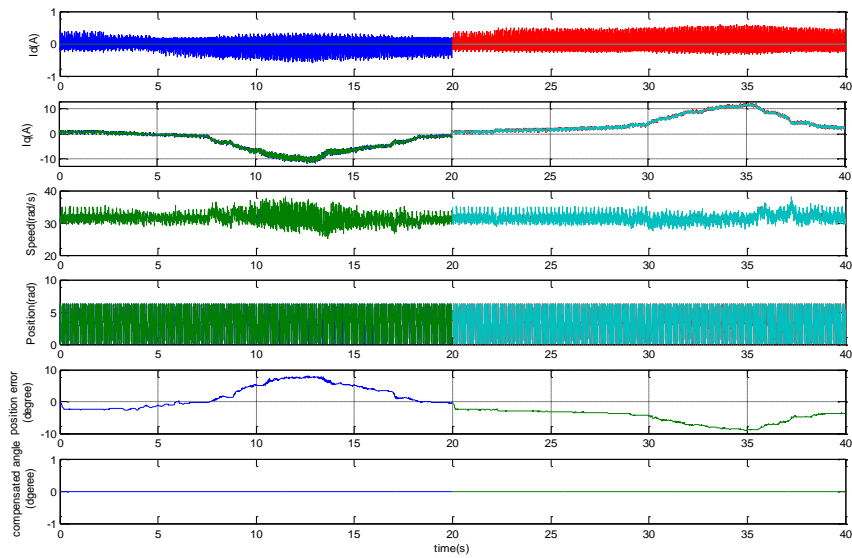


**Figure (11):** position errors at full range of  $I_q$ - no compensation.

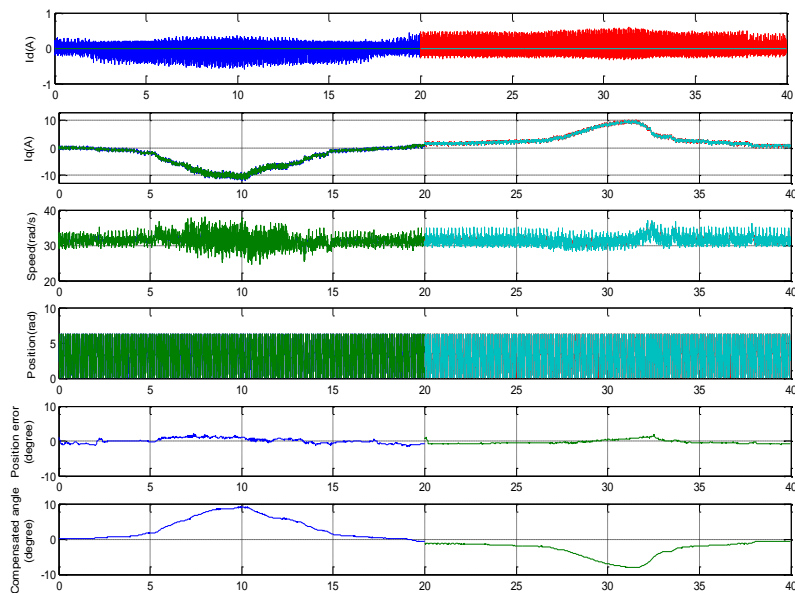


**Figure (12):** position errors at full range of  $I_q$ - with compensation.

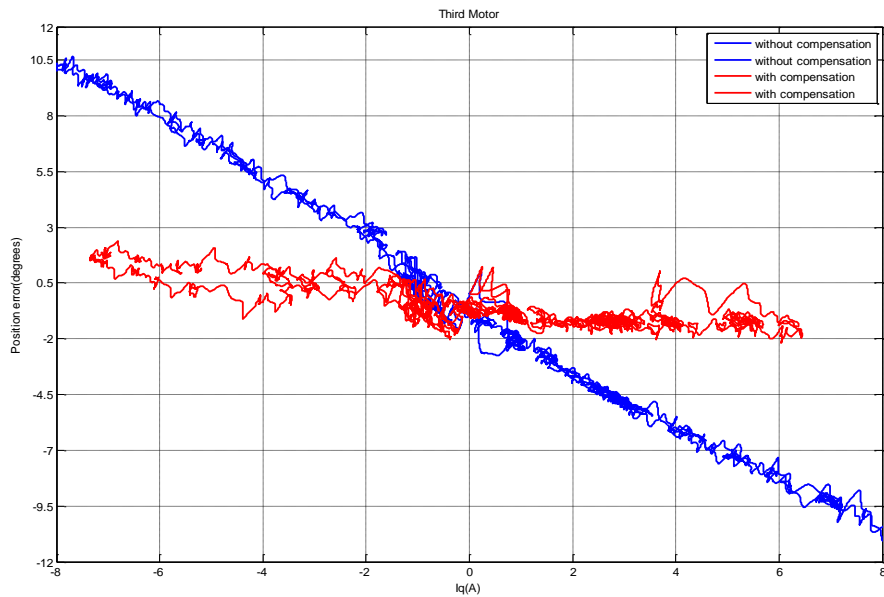


**Figure (13):** Phase shift error between the rotor position and the saliency position before and after compensation using the new method.

### Conclusion

This paper has outlined a new technique for self auto commissioning of sensorless AC drives. The technique includes the measuring of the mechanical parameters of the drive in sensorless mode. This mechanical parameters are used then in automatic tuning of the sensorless speed controller parameters. Also it is used in automatic tuning of the mechanical observer parameters which is important for obtaining a quality estimated speed and positional signals and at the same time not compromising the sensorless dynamic of the drive. And finally the paper has presented a new technique for compensating the position error between the rotor position and the saliency position in permanent magnet motor due to the armature reaction without the need for pre commissioning. It uses the change in  $I_q$  due to the injection of current in  $I_d$  to obtain the compensation angle. The results show a good compensation under sensorless operation. The method also can be used using different injection methods.

## References

- Schauder, C. (1992). *Adaptive Speed Identification for Vector Control of Induction Motors without Rotational Transducers*, IEEE Transactions on Industry Applications, (28), 1054-1061, Oct.
- Jansen, P.L. Lorenz, R.D. (1995). *Transducerless Position and Velocity Estimation in Induction and Salient AC Machines*, IEEE Transactions on Industry Applications, (31), 240–247, Mar.
- Schroedl, M. (1996). *Sensorless Control of AC Machines at Low Speed and Standstill Based on the INFORM Method*. IEEE IAS Annual Meeting, (4), 270-277.
- Sumner, M. Asher, G. (1993). *Autocommissioning for voltage-referenced voltage-fed vector-controlled induction motor drives*. IEE proceedings-B , 140(3). MAY.
- Lorenz, R.D. Van Patten. K.W. (1991). *High-Resolution Velocity Estimation for All-Digital, ac Servo Drives*. IEEE transactions on industry applications, (27), 701 – 705.
- Gao, Q. Asher, G.M. Sumner, M. (2010). *Wide-speed Range Sensorless Control of an AC PM Motor Using the PWM Waveform of a Matrix Converter and without di/dt Sensors*, IEEE Industrial Electronics Society (IECON 2010), Glendale, AZ, USA.
- Hua, Y. Asher, G.M. Sumner, M.Gao, Q. (2007). *Sensorless Control of Surface Mounted Permanent Magnetic Machine Using the Standard Space Vector PWM*, IAS Annual Meeting, 661-667, Sept.
- Arias, A. Sliva, C. Asher, G. Clare, J. Wheeler, P. (2006). *Use of a Matrix Converter to Enhance the Sensorless Control of a Surface-Mount Permanent-Magnet AC Motor at Zero and Low Frequency*. IEEE Transactions on Industrial Electronics, 53(2). April.
- Holtz, J. (2008). *Acquisition of Position Error and Magnet Polarity for Sensorless Control of PM Synchronous Machines*. IEEE Transactions on Industry Applications, (44), 1172–1180.

- Ha, J.-I. Sul, S.-K. (1997). Sensorless field orientation of an induction machine by high frequency signal injection, *IEEE IAS Annual Meeting*, (5), 426–432.
- Corley, M. Lorenz, R.D. (1998). *Rotor Position and Velocity Estimation for a Salient-Pole Permanent Magnet Synchronous Machines at Standstill and High Speeds*. IEEE Transactions on Industry Applications, (34), 784–789.